

Circuit with small-capacitance high-quality Nb Josephson junctions

Michio Watanabe*

Frontier Research System, RIKEN, 2-1 Hirosawa, Wako, Saitama 351-0198, Japan

Yasunobu Nakamura and Jaw-Shen Tsai

NEC Fundamental Research Laboratories, 34 Miyukigaoka, Tsukuba, Ibaraki 305-8501, Japan
and Frontier Research System, RIKEN, 2-1 Hirosawa, Wako, Saitama 351-0198, Japan

(Dated: September 19, 2003)

We have developed a fabrication process for nanoscale tunnel junctions which includes focused-ion-beam etching from different directions. By applying the process to a Nb/(Al-)Al₂O₃/Nb trilayer, we have fabricated a Nb single-electron transistor (SET), and characterized the SET at low temperatures, $T = 0.04 - 40$ K. The superconducting gap energy and the transition temperature of the Nb SET agree with the bulk values, which suggests high quality Nb junctions. The single-electron charging energy of the SET is estimated to be larger than 1 K.

Appl. Phys. Lett. **84**, 410 (2004) [DOI: 10.1063/1.1640798]

Circuits with Josephson tunnel junctions are one of the most promising candidates for quantum bits (qubits) for quantum computation in solid-state electronic devices.^{1,2} The Josephson junctions (JJs) for qubits should have large subgap resistance and an appropriate E_J/E_C ratio, where E_J is the Josephson energy and E_C is the charging energy of the junction. The desired range of E_J/E_C depends on the degree of freedom (charge, flux, or phase) to be controlled in the circuit. For cases of charge qubit³ and flux qubit,⁴ a typical junction size is on the order of $0.1 \times 0.1 \mu\text{m}^2$, for which the fabrication technique of Josephson tunnel junctions has been well established only for Al/Al₂O₃/Al junctions. However, materials with larger superconducting gap energy Δ , e.g., Nb ($\Delta_{\text{Nb}}/\Delta_{\text{Al}} \approx 8$), are more attractive especially for flux qubits, where one wants to have large E_J/E_C and keep E_C sufficiently larger than the thermal energy $k_B T$. Note that E_J is proportional to Δ .

There have been a number of attempts to fabricate small-capacitance Al/Al₂O₃/Nb or Nb/(Al-)Al₂O₃/Nb JJs.^{5,6,7,8,9,10} Conventional nanoscale fabrication processes based on *e*-beam lithography and multiangle shadow evaporation, which work fine for Al/Al₂O₃/Al JJs, tend to deteriorate the quality of Nb, i.e., Δ and the superconducting temperature T_c are reduced considerably (a summary of this can be found in Fig. 1 of Ref. 10). Rather large values of Δ_{Nb}/e have been obtained in single junctions fabricated by a sloped-edge technique⁵ (1–1.2 mV) and in a single-electron transistor (SET) fabricated by a multilayer technique⁷ (1.35 mV). However, it would be difficult to fabricate multijunction devices using the sloped-edge technique, and the charging energy of the SET fabricated by the multilayer technique was ≈ 0.15 K, which might be acceptable for flux qubits

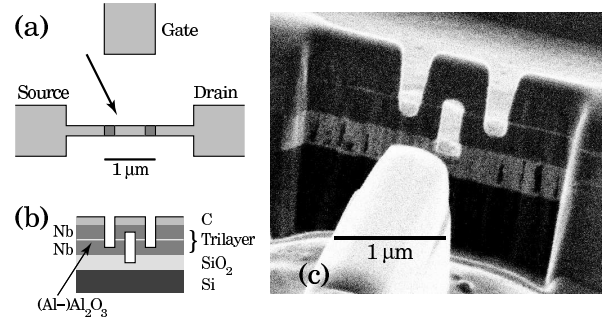


FIG. 1: Nb single-electron transistor. (a) Top view. (b) Side view. (c) Focused-ion-beam secondary-electron image taken from the direction shown in (a).

but would be too small for charge qubits and for most single-electron-tunneling devices.

We have developed a process to fabricate high-quality small-capacitance Nb/(Al-)Al₂O₃/Nb JJs which includes focused-ion-beam (FIB) etching from two different directions. By employing the process, we have fabricated SETs with a three-dimensional structure, shown in Fig. 1. Details of the process are as follows. A trilayer of Nb (thickness: $0.3 \mu\text{m}$), Al ($0.01 \mu\text{m}$)–Al₂O₃ (≈ 1 nm), and Nb ($0.3 \mu\text{m}$) was sputtered onto a SiO₂/Si substrate in a single vacuum cycle. The Al₂O₃ layer was formed by oxidizing the surface of Al. The film was then patterned with standard photolithography and Ar⁺ milling, where the smallest feature size in this step was $\approx 5 \mu\text{m}$. The dimensions of the trilayer were decreased further in a Ga⁺ FIB system, which has three functions: deposition, etching, and observation. From the direction perpendicular to the substrate, we first deposited C (thickness: $\approx 0.1 \mu\text{m}$) by decomposing phenanthrene (C₁₄H₁₀) gas with a Ga⁺ beam current of 48 pA. The role of the C layer is to minimize damage of the trilayer by Ga⁺ during the etching process described below. Then, we etched into the pattern shown in Fig. 1(a) except for the fine structure on the narrow track between the source

*Present address: National Institute of Standards and Technology, Division 817, 325 Broadway, Boulder, CO 80305; electronic mail: watanabe@boulder.nist.gov

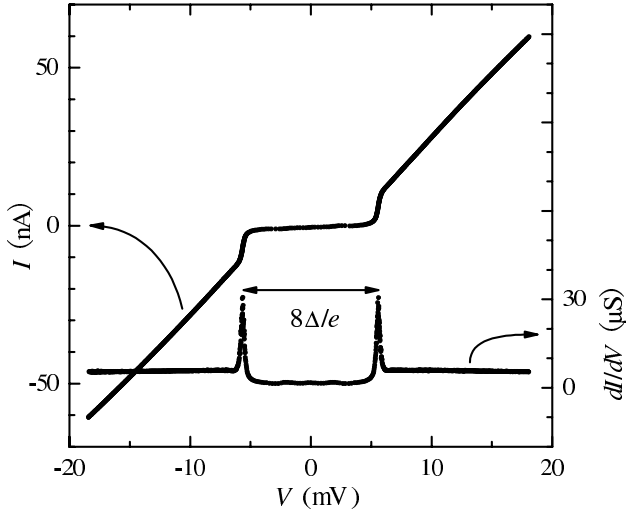


FIG. 2: Current-voltage characteristics (upper data set) and the differential resistance vs bias voltage V (lower data set) of the Nb single-electron transistor at $T = 3.2$ K.

and the drain. For etching, we used two beam currents, 1.3 nA (rough etching) and 9 pA, not only for efficiency but also to minimize the amount of material redeposited on the sides of the narrow track. After tilting the substrate $\approx 88^\circ$, three holes were made with a 9 pA beam current on the side of the track as shown in Fig. 1(b). A double-junction structure formed between the holes. An example of the SET fabricated in the above process is shown in Fig. 1(c), which is a secondary-electron image taken in the same FIB system. The final step in our fabrication process is anodization, and there are two reasons for this. One is to eliminate completely short circuit of the junction due to conducting materials (mostly Nb) redeposited during FIB etching, by changing the conducting materials into insulating oxides. The other is to suppress the contribution of the sample surface, which might have been damaged by Ga^+ , to electrical conduction. Because anodization also reduces the effective area of the junctions, we designed the initial junction size delineated by the FIB to be $> 0.2 \times 0.2 \mu\text{m}^2$, although we could fabricate much smaller junctions by this technique. We kept the anodization current constant at a value in the range 1–10 $\mu\text{A}/\text{cm}^2$ and, for the sample discussed below, we anodized up to 60 V, which reduced the effective junction area to $< 0.1 \times 0.1 \mu\text{m}^2$. The FIB etching was quite reproducible, although the resistance of the SET after anodization varied from sample to sample.

We measured the samples in a ^4He continuous-flow cryostat with a Si-diode thermometer mounted next to the sample holder. The current-voltage (I - V) characteristics of one of the samples at $T = 3.2$ K is shown in Fig. 2. The I - V curve exhibits a sharp superconducting gap, whose value corresponds to two Nb JJs. We obtained $\Delta_{\text{Nb}}/e = 1.4$ mV from the distance between the peaks in the differential conductance dI/dV vs V curve (see the lower data set of Fig. 2). Here the charging en-

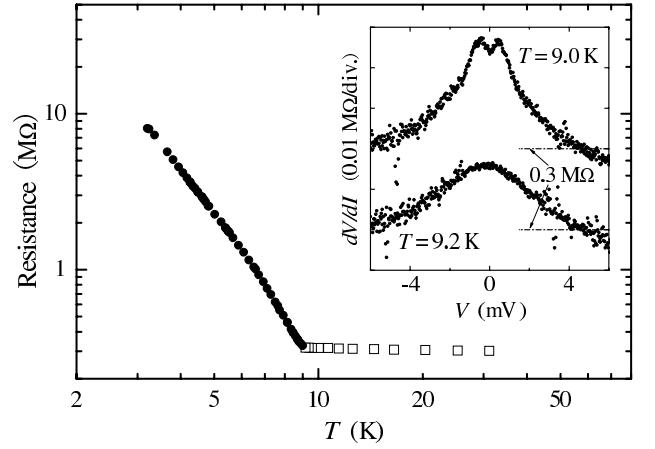


FIG. 3: Temperature dependence of the zero-bias resistance at $T \geq 9.2$ K (open squares) and that of the subgap resistance at $T \leq 9.0$ K (closed circles). Inset: Differential resistance vs bias voltage at $T = 9.0$ and 9.2 K. The origin of the vertical axis is offset for each curve for clarity.

ergy of the SET is negligibly small for the estimate of Δ_{Nb} as will be discussed later. This value of 1.4 mV is the largest for $\sim 0.1 \times 0.1 \mu\text{m}^2$ junctions. Moreover, it agrees with the values at liquid ^4He temperatures for 1–10 μm scale JJs fabricated by a standard photolithographic technology for integrated JJ circuits. We also measured the temperature dependence of the I - V curve in order to determine T_c . The I - V curve looks almost linear at $T > 8$ K. However, when we look at the differential resistance dV/dI , it is easy to find a qualitative difference between the dV/dI vs V curves at $T \leq 9.0$ K and those at $T \geq 9.2$ K. The inset of Fig. 3 shows the dV/dI vs V curve at $T = 9.0$ and 9.2 K. The curve at 9.0 K has a dip in the middle, while that at 9.2 K does not. Based on this qualitative difference, we determine that $T_c = 9.1 \pm 0.2$ K, which agrees with the bulk value of 9.2 K within the error. Here ± 0.2 K includes all errors in thermometry and T_c determination. We confirm the adequacy of the above T_c determination in Fig. 3 by plotting versus T the zero-bias resistance for $T \geq 9.2$ K (normal state) and the subgap resistance for $T \leq 9.0$ K (superconducting state), where we have defined the subgap resistance as the maximum value of $V/I(V)$. From the values of Δ and T_c , we conclude that the quality of our JJs is high and it has not deteriorated in the FIB etching process.

Let us look at the properties of the sample as an SET. The gate electrode is located $> 1 \mu\text{m}$ from the double-junction system (Fig. 1), and the voltage V_g applied to the gate modulates the current even up to 5 K (data not shown). Thus, the sample indeed works as an SET. In order to characterize the sample further, we cooled it down to 0.04 K in a ^3He - ^4He dilution refrigerator. At $T \leq 1$ K, the subgap resistance becomes $> 10^2$ M Ω , which is significantly larger than the normal-state resistance, 0.3 M Ω , and again, suggests high quality junctions.

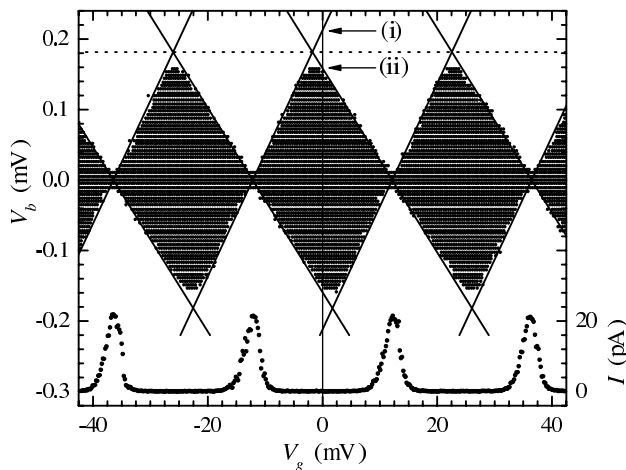


FIG. 4: Blockade of single-electron tunneling in the normal state ($B = 2.7$ T) at $T = 0.05$ K. Lower data set: Current I vs gate voltage V_g at $V = 0.026$ mV, where V is the bias voltage. Upper data set: Region of $|I| < 10$ pA on the V_g - V plane. The closed diamonds indicate the Coulomb-blockade region. The horizontal dotted line corresponds to $2E_C/e$, where E_C is the single-electron charging energy of the SET.

The parameters of a SET, such as the capacitances C_1 and C_2 of the tunnel junctions and the capacitance C_g between the island electrode and the gate electrode, can be determined by measuring the blockade of single-electron tunneling in the normal state at a low enough temperature.¹¹ We drove the Nb SET into the normal state by applying a magnetic field of 2.7 T perpendicular to the substrate, and measured I - V_g curves for different values of V at $T = 0.05$ K. An example of the I - V_g curve, which is for $V = 0.026$ mV, is shown in the lower data set of Fig. 4. One period in the V_g axis corresponds to e/C_g , so that $C_g = 7$ aF, which is consistent with the geometry. In the upper data set of Fig. 4, we estimate the zero-current region at $T = 0$ on the V - V_g plane (Coulomb diamond). The horizontal dotted line corresponds to $2E_C/e$ of the SET. Thus, from $2E_C/e = 0.18$ mV in Fig. 4, we obtain $E_C/k_B = 1.1$ K, which is consistent with the effective junction area of $< 0.1 \times 0.1 \mu\text{m}^2$ and sufficiently larger than the base temperature of a typical dilution refrigerator, < 0.1 K. When $C_g \ll C_1, C_2$, which is the case in our Nb SET, C_1 and C_2 are estimated from the slopes of the solid lines in Fig. 4. We find that $C_1/C_2 = 0.75$, although we designed it so that $C_1 = C_2$.

The reason for asymmetry in the junction capacitance is that we had to anodize the SET up to a large voltage in

order to eliminate the short circuit. The accuracy of the capacitances could be improved by introducing a step of reactive-gas-assisted etching at the end of the FIB process. We have already confirmed that XeF_2 gas enhances the etching rate of Nb $\approx 10^2$ times and “cleans up” redeposited Nb. By introducing the step, we would be able to reduce the anodization voltage considerably. Reducing the anodization voltage would also improve the yield of the fabrication process.

It should be noted that our process is also applicable to more complex circuits. Moreover, it is much more flexible in terms of circuit pattern than the conventional technique based on e -beam lithography and shadow evaporation, or the multilayer technique in Ref. 7. Very recently, a similar FIB-etching technique was independently developed, and nanoscale single junctions with a variety of materials were fabricated.¹² Thus, the process is not limited to Nb/(Al-)Al₂O₃/Nb junctions.

In the superconducting state, one expects that the supercurrent flowing through the SET depends on V_g periodically¹³ and that the period is $2e/C_g$ ($2e$ periodic). In many experiments, however, a period of e/C_g (e periodic), which suggests the existence of subgap quasiparticle states,¹³ has also been seen. In small-capacitance Al/Al₂O₃/Nb or Nb/(Al-)Al₂O₃/Nb systems, only e periodicity has been reported. In our Nb SET, the measured supercurrent at $T = 0.04$ K and $B = 0$ is also e periodic, and its magnitude is on the order of 10 pA, which is $\approx 10^{-3}$ the theoretical maximum, $\sim I_0/2$, where $I_0 \equiv \pi\Delta/2eR_n$ is the Ambegaokar-Baratoff critical current and R_n is the normal-state resistance of the junction. Further investigation of the periodicity by measuring high-quality Nb SETs with different parameters would clarify whether the e periodicity is intrinsic to Nb or not.

In summary, we have fabricated a high-quality Nb SET with $E_C/k_B > 1$ K by developing a fabrication process for nanoscale tunnel junctions. The process is much more flexible than conventional ones based on e -beam lithography.

The authors are grateful to Y. Kitagawa for preparation of the Nb/(Al-)Al₂O₃/Nb trilayer, to M. Ishida for assistance with the FIB system, to H. Akaike for valuable comments on anodization, and to Yu. Pashkin, T. Yamamoto, and O. Astafiev for fruitful discussions. This work was supported in part by the Special Postdoctoral Researchers Program of RIKEN and by MEXT.KAKENHI (Grant No. 15740190).

¹ Yu. Makhlin, G. Schön, and A. Shnirman, Rev. Mod. Phys. **73**, 357 (2001).

² R. Fitzgerald, Phys. Today **55**, (6), 14 (2002).

³ Y. Nakamura, Yu. A. Pashkin, and J. S. Tsai, Nature (London) **398**, 786 (1999).

⁴ I. Chiorescu, Y. Nakamura, C. J. P. M. Harmans, and J. E. Mooij, Science **299**, 1869 (2003).

⁵ J. M. Martinis and R. H. Ono, Appl. Phys. Lett. **57**, 629 (1990).

⁶ Y. Harada, D. B. Haviland, P. Delsing, C. D. Chen, and

- T. Claeson, Appl. Phys. Lett. **65**, 636 (1994).
- ⁷ A. B. Pavolotsky, T. Weimann, H. Scherer, V. A. Krupenin, J. Niemeyer, and A. B. Zorin, J. Vac. Sci. Technol. B **17**, 230 (1999).
- ⁸ N. Kim, K. Hansen, J. Toppari, T. Suppula, and J. Pekola, J. Vac. Sci. Technol. B **20**, 386 (2002).
- ⁹ R. Dolata, H. Scherer, A. B. Zorin, and J. Niemeyer, Appl. Phys. Lett. **80**, 2776 (2002).
- ¹⁰ R. Dolata, H. Scherer, A. B. Zorin, and J. Niemeyer, J. Vac. Sci. Technol. B **21**, 775 (2003).
- ¹¹ G.-L. Ingold and Yu. V. Nazarov, in *Single Charge Tunneling*, edited by H. Grabert and M. H. Devoret (Plenum, New York, 1992), chap. 2.
- ¹² C. Bell, G. Burnell, D.-J. Kang, R. H. Hadfield, M. J. Kappers, and M. G. Blamire, Nanotechnology **14**, 630 (2003).
- ¹³ P. Joyez, Ph.D. thesis, Univ. of Paris 6, Paris France (1995).